CHAPTER IV
RESULTS AND DISCUSSION

4.1 Characterization of poly(S/DVB)HIPEs

4.1.1 Effect of type of salt

SEM micrographs (Figure 4.1) show morphological characteristics of poly(styrene/divinylbenzene)HIPEs filled with different type of stabilizing salt.

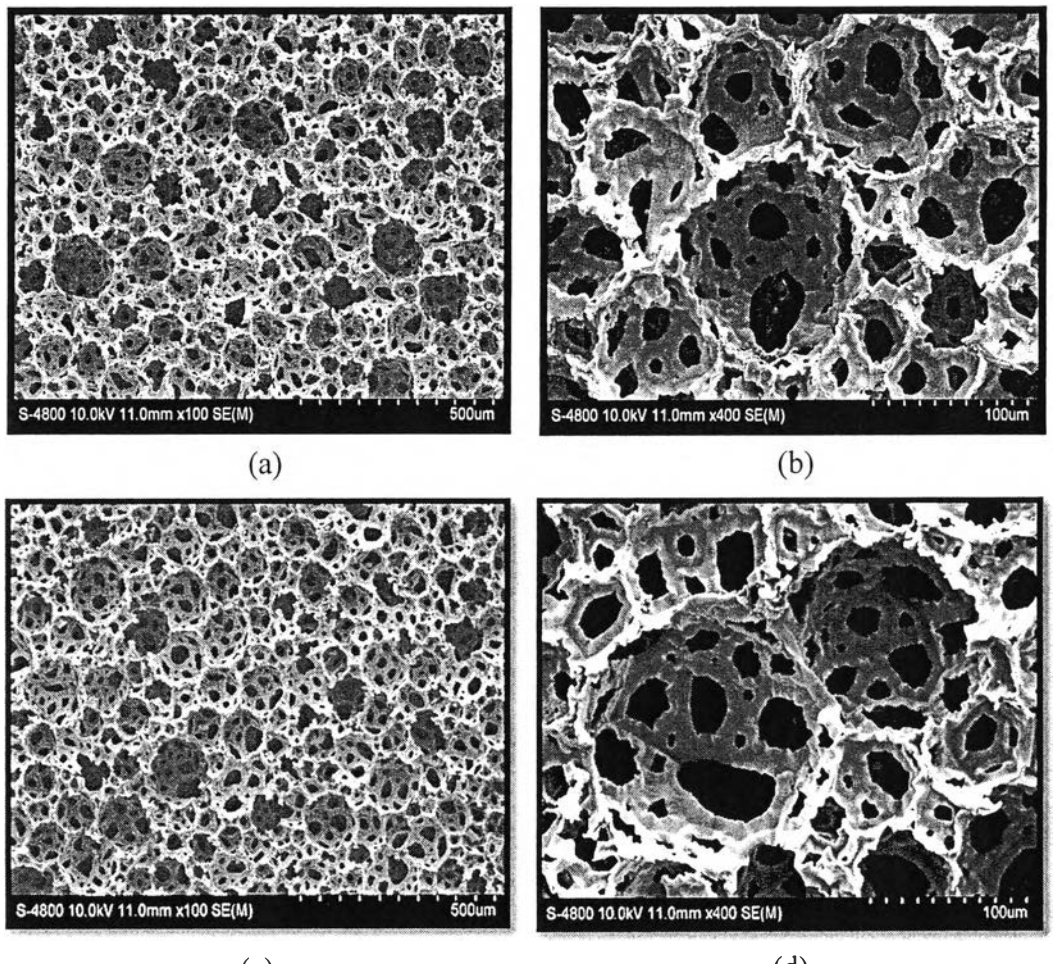

Figure 4.1 SEM micrographs of poly(S/DVB)HIPEs filled with different type of stabilizing salt ; (a,b) $CaCl_2$ and (c,d) NaCl with two different magnifications ×100 and ×400.

Table 4.1 Relative equilibrium water adsorption capacities and pore sizes characteristics of $CaCl_2$- and NaCl-polyHIPEs

Salt	Relative equilibrium water adsorption capacity (g/g)	Pore size (μm)
$CaCl_2$	12.12±0.07	88
NaCl	12.41±0.16	90

The Addition of salt into the system can enhance the rigidity of the interfacial film in W/O HIPEs, because of the presence of ordered structure by surfactant head groups packing, leading to stability of polyHIPE system (Pons *et al.*, 1992). The salts can also enhance stability by inhibiting Ostwald ripening, a process by which large droplets grow at the expense of smaller ones. Furthermore, they reduce the solubility of the aqueous phase in the oil phase, thus reducing the attractive forces between the droplets (Kizling *et al.*, 1992).

Poly(S/DVB)HIPEs were prepared by using an oil:aqueous phase; 10:90 ratio by volume, S:DVB; 80:20 ratio by volume and span80, a surfactant with low HLB balance (HLB 4.3) could act as the most suitable surfactant to provide stable emulsion for poly(S/DVB)HIPE system (Williams *et al.*, 1991). The pore sizes and interconnected pore sizes were found similar to each other with different type of salt furthermore, they also had opened cell and highly interconnected structure. $CaCl_2$ and NaCl foams had average pore diameter around 88 μm and 90 μm respectively. The water adsorption characteristics of poly(S/DVB)HIPEs were studied by immersing in DI water, then calculate with equation (1), until the equilibrium adsorption would be obtained. As shown from the Table 4.1, NaCl-polyHIPE provided water adsorption capacity similar to $CaCl_2$-polyHIPE.

4.1.2 Effect of oil:aqueous phase ratio by volume

SEM micrographs (Figure 4.2) show morphological characteristics of poly(S/DVB)HIPEs varied with increasing in aqueous ratio.

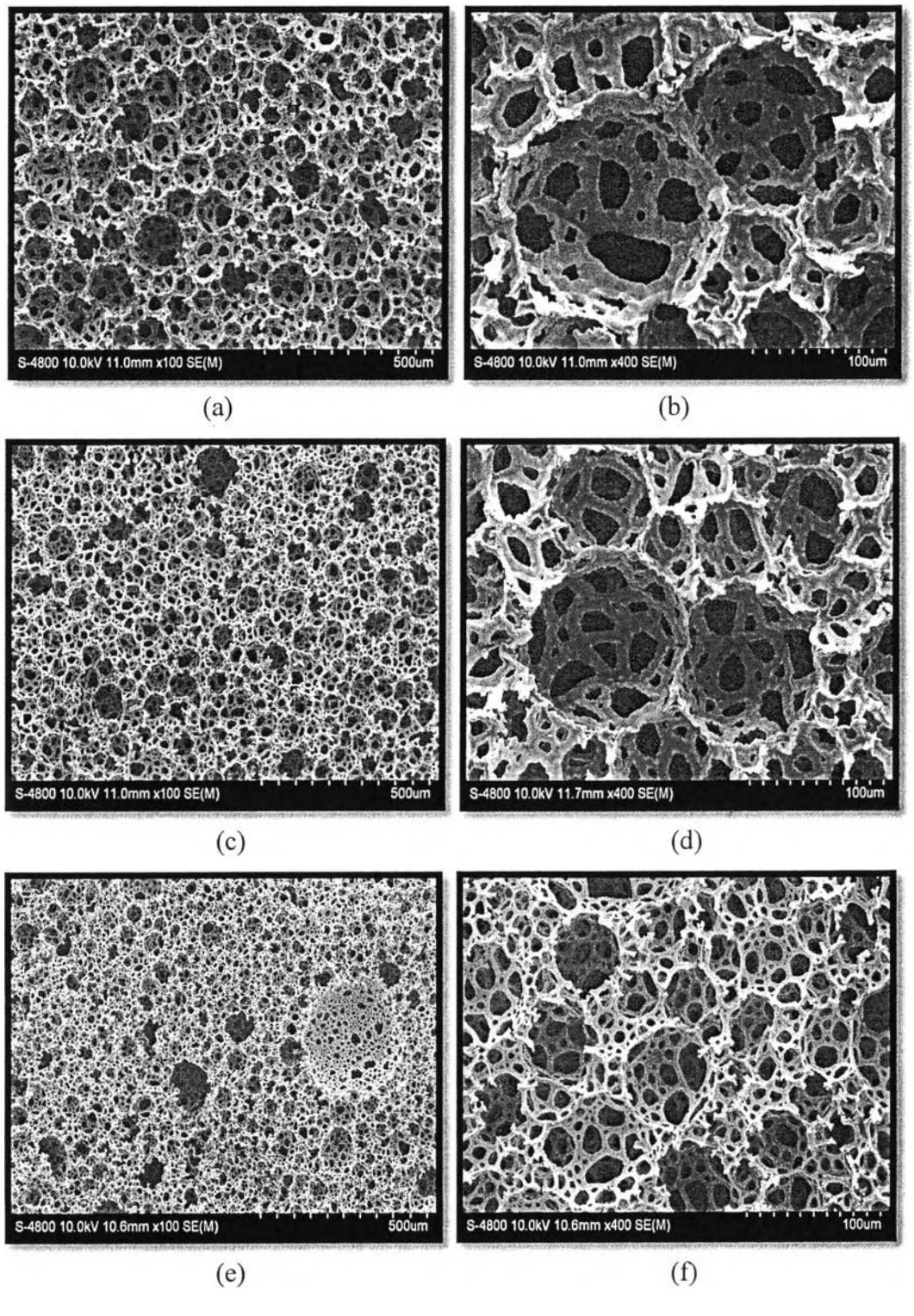

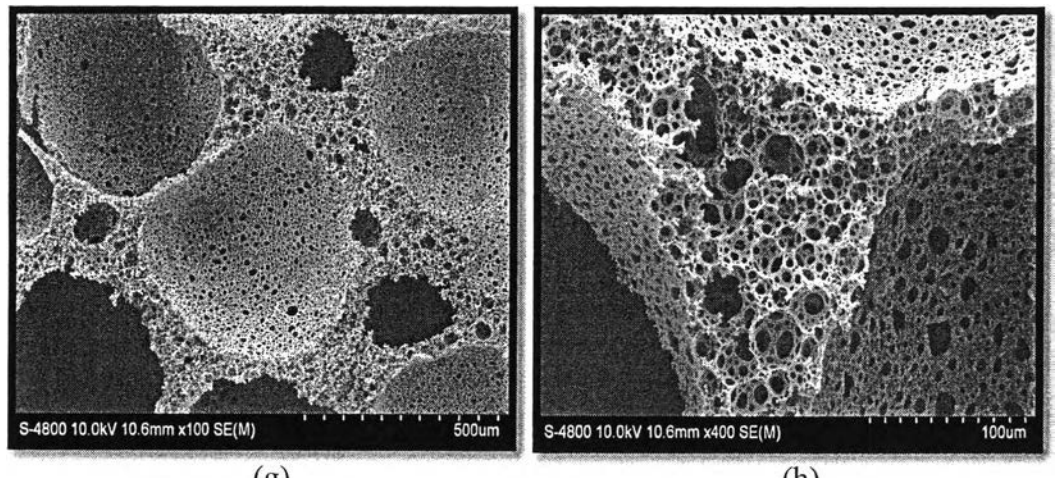

(g) (h)

Figure 4.2 SEM micrographs of poly(S/DVB)HIPEs varied with oil:aqueous phase ratio by volume ; (a,b) 10:90 ; (c,d) 8:92 ; (e,f) 6:94 and (g,h) 4:96 polyHIPEs with two different magnifications ×100 and ×400.

Table 4.2 Surface areas and pore sizes characteristics of varied oil:aqueous phase ratio poly(S/DVB)HIPEs

Oil:aqueous phase	Surface areas (m^2/g)	Pore size (μm)
10:90	223.612	90
8:92	21.847	67
6:94	18.005	42
4:96	50.582	20

Poly(S/DVB)HIPEs were prepared by fixing S:DVB; 80:20 ratio by volume and using NaCl as a stabilizing salt. The average pore diameters decreased with increasing in aqueous phase ratio. In addition, it was clear from these micrographs that the 10:90 and 8:92 poly(S/DVB)HIPEs did not have coalescence pores, whereas the 6:94 and 4:96 poly(S/DVB)HIPEs had large coalescence pores which diameters were about 300 μm and 500 μm respectively. Moreover, increasing in aqueous phase ratio provided more opened cell porous structures (Figure 4.2b, d, f and g) (Williams *et al.*, 1990).

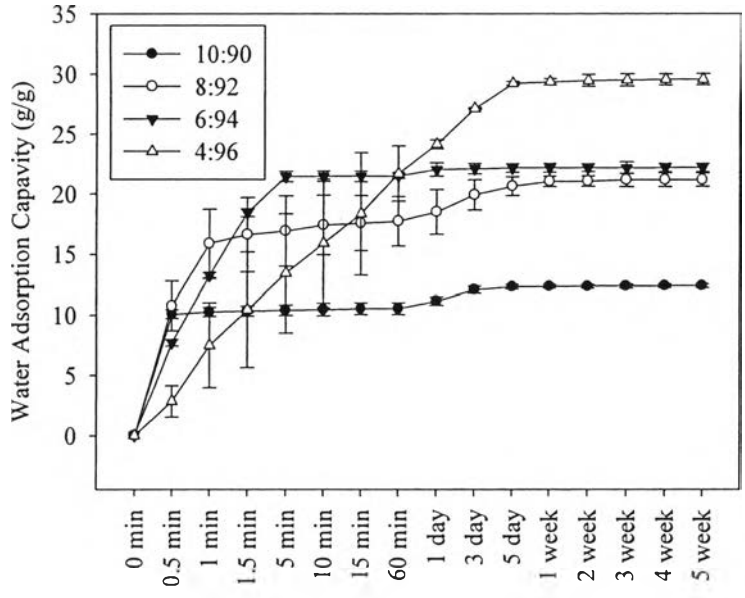

Figure 4.3 Water adsorption capacities of poly(S/DVB)HIPEs varied with oil:aqueous phase ratio by volume with interval time.

From assumption, the high aqueous phase ratio was expected to get large pore size and thus, would enhance water adsorption capacity. The explanation for these results was found in the changes of the cell structure. The high aqueous phase ratio poly(S/DVB)HIPE did not generate the larger pore size but, rather provided the smaller pores and more some coalescence pores because, experimentally, the more increasing in aqueous phase ratio, the more phase separation happened owing to Ostwald ripening phenomena (Kabalnov *et al.*, 1987). The pore size showed agreeably to surface areas, except the 10:90 poly(S/DVB)HIPEs which provided different from trend. This could be possible if it is assumed that the random polymerization of styrene/divinylbenzene had been occurred, because styrene and divinylbenzene were mixed together at the same time before adding initiator. Due to the similar reactivities of styrene monomer and divinylbenzene monomer (Vieweg *et al.*, 1969 and Claudio *et al.*, 2008), polymerization might occur randomly which could generate random cell structure, thus, it was possible to have an error of surface area analysis. The 4:96 oil:aqueous ratio poly(S/DVB)HIPE obtained maximum water uptake around 29.57 g/g (Figure 4.3) as the result of the spongy form characteristic (Figure 4.2g) which allowed more swelling than the other rigid forms (Burke *et al.*, 2010). A further reason is

increasing in aqueous phase resulting in less hydrophobicity which led the materials could attach more water.

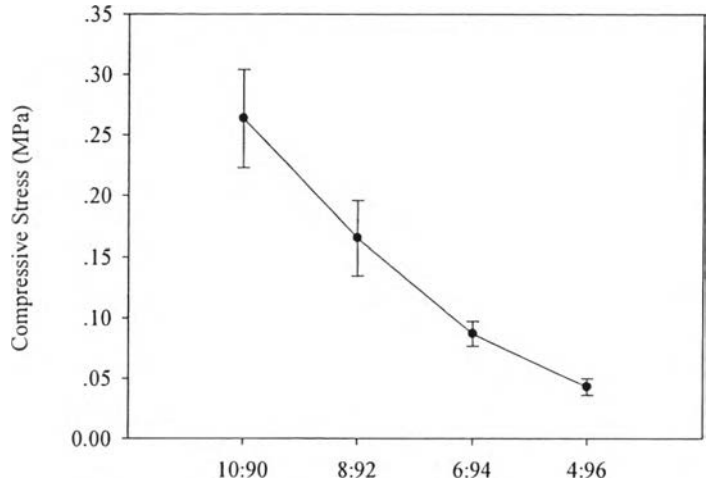

Figure 4.4 Compressive stress of poly(S/DVB)HIPEs varied with oil:aqueous phase ratio by volume.

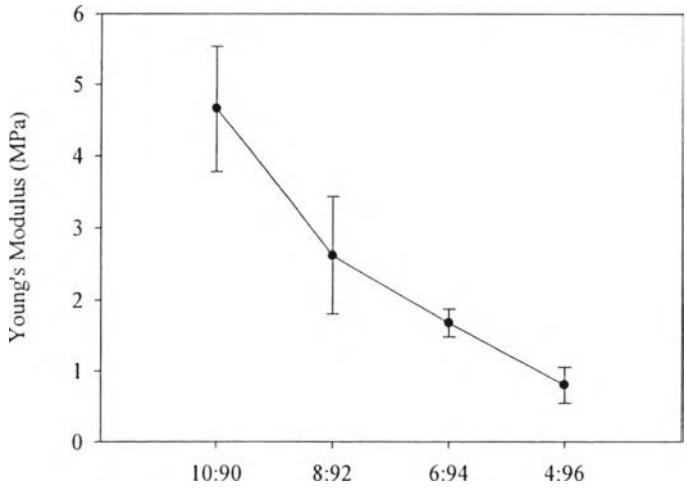

Figure 4.5 Young's modulus of poly(S/DVB)HIPEs varied with oil:aqueous phase ratio by volume.

Figure 4.4 and 4.5 shows the compressive stress and Young's modulus of poly(S/DVB)HIPEs varied with oil:aqueous phase ratio by volume (10:90 to 4:96), impairing the compressive stress from 0.2635 to 0.0430 MPa and Young's modulus from 4.6579 to 0.8003 MPa. In other words, the increasing in aqueous phase resulted in the decreasing compressive stress and Young's modulus

due to the increases of the coalescence pores which influence on changing material from the rigid form to the spongy form (Burke *et al.*, 2010).

4.1.3 Effect of degree of crosslinking monomer of poly(S/DVB)HIPEs

SEM micrographs (Figure 4.6) show morphological characteristics of poly(S/DVB)HIPEs varied with increasing in DVB content.

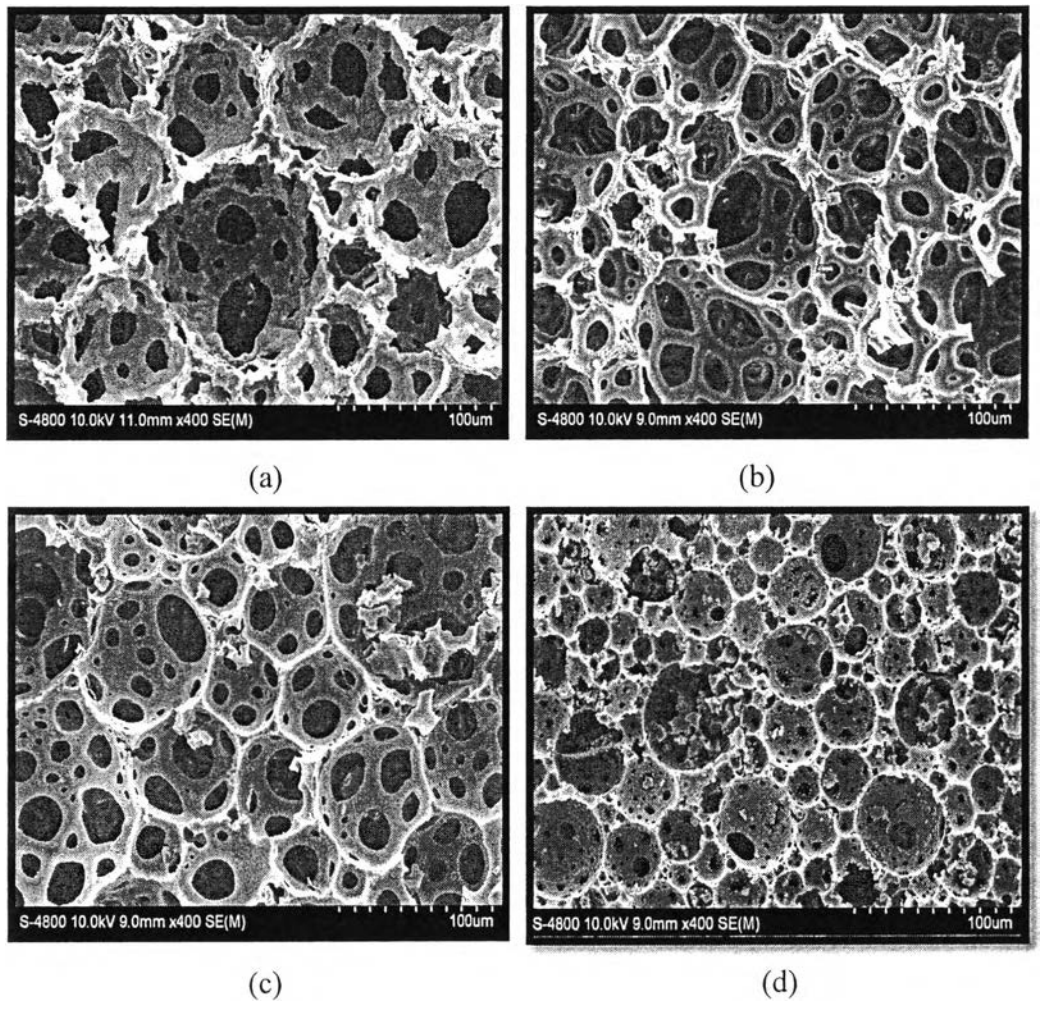

Figure 4.6 SEM micrographs of poly(S/DVB)HIPEs varied with S:DVB ratio by volume; (a) 80:20; (b) 70:30; (c) 60:40 and (d) 0:100 poly(S/DVB)HIPEs with magnification ×400.

Table 4.3 Surface areas and pore sizes characteristics of varied S:DVB ratio poly(S/DVB)HIPEs

S:DVB	Surface areas (m^2/g)	Pore size (μm)
80:20	8.585	88
70:30	7.767	65
60:40	9.474	60
0:100	28.018	34

Poly(S/DVB)HIPEs were prepared by fixing oil:aqueous phase; 10:90 ratio by volume and using $CaCl_2$ as a stabilizing salt. The average pore diameters were found to decrease dramatically when the DVB level increases. Obviously, the porous structure showed rough surface at low degree of DVB, a crosslinking comonomer (Figure 4.6a) because the structure could pack more flexible than poly(S/DVB)HIPEs at high degree of DVB.

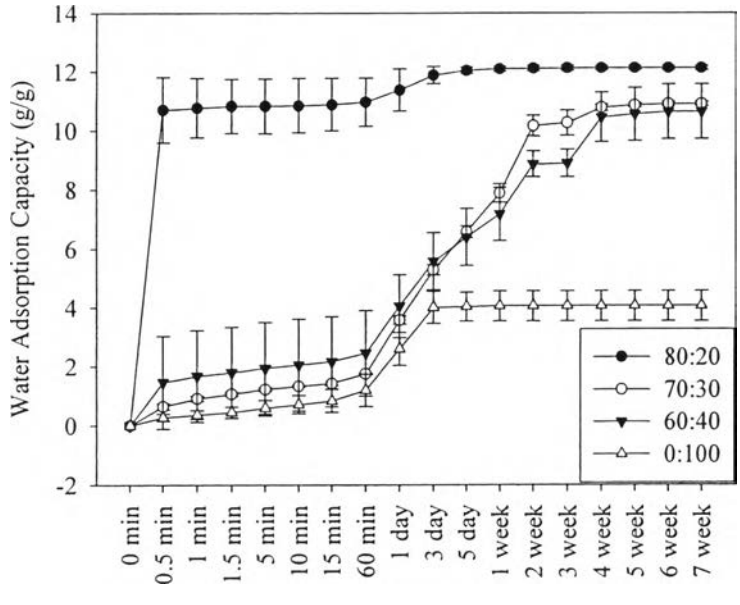

Figure 4.7 Water adsorption capacities of poly(S/DVB)HIPEs varied with S:DVB ratio by volume with interval time.

The DVB content directly affected the water adsorption of poly(S/DVB)HIPEs. According to the Figure 4.7, interestingly, the water adsorption capacity was not influenced by surface areas but it was liable that as increasing degree of crosslinking monomer, the water uptake went down. Theoretically, the swelling of the material is dependent on the nature and concentration of the cross-linking monomer (Rao *et al.*, 2011). In this case, the DVB monomer had inhibited swelling of material by forming cross-linked networks during polyHIPE formation. With increasing in DVB content, the structure exhibited more rigid form, thus, resulting in less swelling of material. Moreover, another interested reason is from the pore size which might have an effect to the water adsorption capacity as well. As seen from Figure 4.7, the 80:20 S:DVB ratio poly(S/DVB)HIPE which had the biggest pore size adsorbed a lot of water immediately after immersing just 30 seconds.

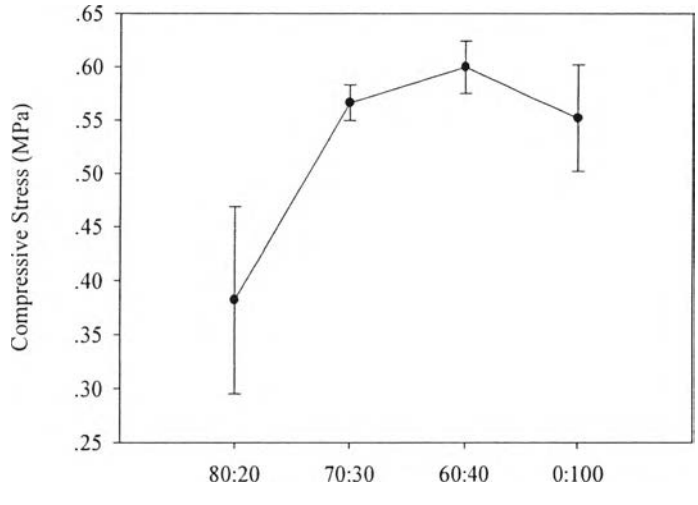

Figure 4.8 Compressive stress of poly(S/DVB)HIPEs varied S:DVB ratio.

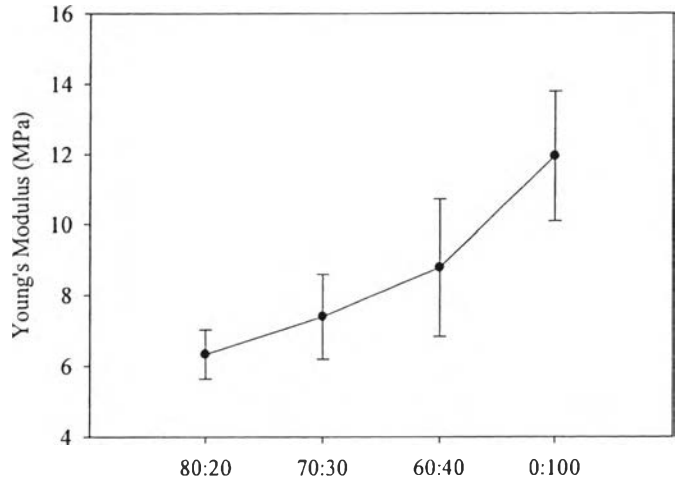

Figure 4.9 Young's modulus of poly(S/DVB)HIPEs varied S:DVB ratio.

Figure 4.8 and 4.9 shows the compressive stress and Young's modulus of poly(S/DVB)HIPEs varied S:DVB ratio, increasing in DVB content from 20% to 100% could enhance the Young's modulus from 6.3344 to 11.9476 MPa and compressive stress from 0.3820 to 0.5997 MPa but, went down to 0.5519 MPa at 100%DVB because the resultant foam were very crispy. The overall results can explain that the increasing DVB content resulted in the increasing compressive stress and Young's modulus owing to the increase of degree of crosslinking.

4.2 Characterization of poly(S/EGDMA)HIPEs

4.2.1 Effect of degree of crosslinking monomer of poly(S/EGDMA)HIPEs

SEM micrographs (Figure 4.10) show morphological characteristics of poly(S/EGDMA)HIPEs varied with increasing in EGDMA content.

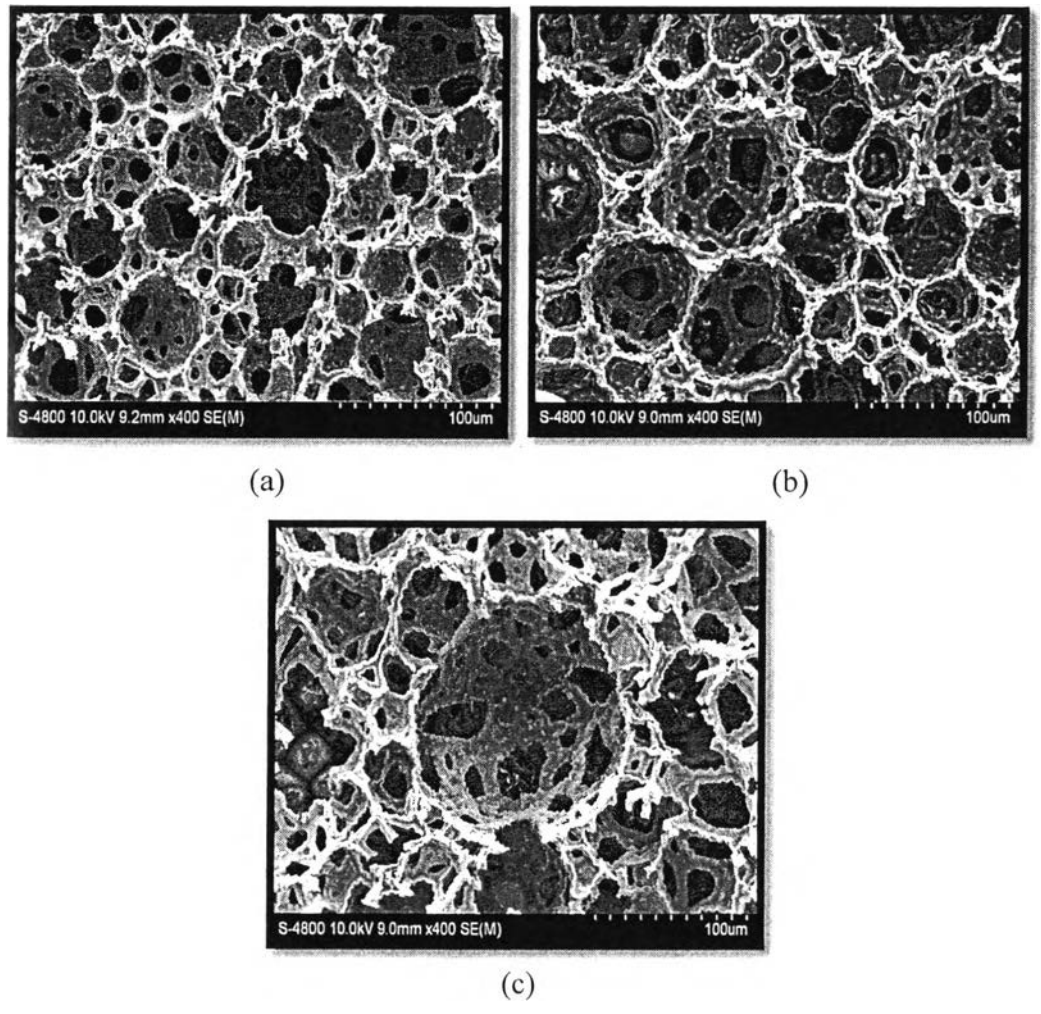

Figure 4.10 SEM micrographs of poly(S/EGDMA)HIPEs varied with S:EGDMA ratio by volume; (a) 80:20; (b) 70:30 and (c) 60:40 poly(S/EGDMA)HIPEs with magnification ×400.

Table 4.4 Surface areas and pore sizes characteristics of varied S:EGDMA ratio poly(S/EGDMA)HIPEs

S:EGDMA	Surface areas (m^2/g)	Pore size (μm)
80:20	71.207	61
70:30	13.873	65
60:40	5.100	89

Poly(S/EGDMA)HIPEs were prepared by fixing oil:aqueous phase; 10:90 ratio by volume and using $CaCl_2$ as a stabilizing salt. The average pore diameters were found to increase with increase in EGDMA level (Table 4.4). This resulted from destabilization through droplet coalescence and/or Ostwald ripening by addition of more EGDMA, a hydrophilic component, to the organic phase of a HIPE (Livshin *et al.*, 2008). However, increasing in droplet size, the amount of interconnected holes inversely decreased. This means the openness and interconnectivity of the porous structure decreased with increasing EGDMA content (Figure 4.10).

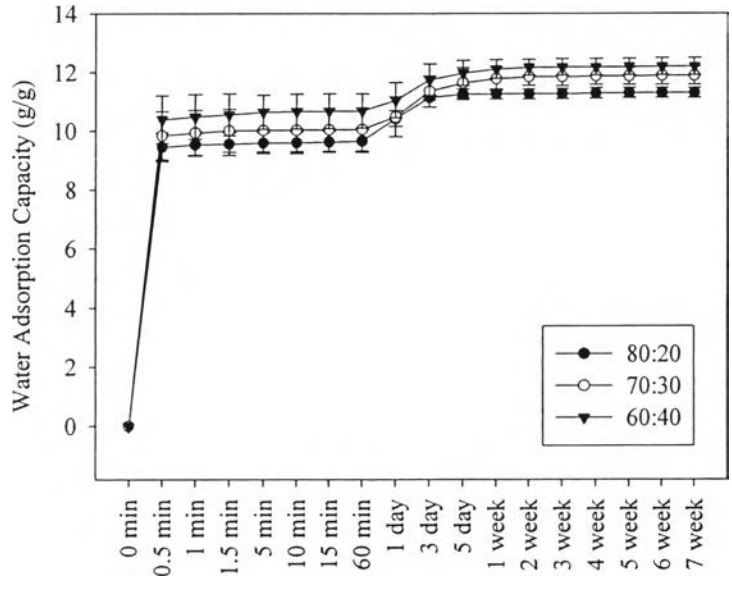

Figure 4.11 Water adsorption capacities of poly(S/EGDMA)HIPEs varied with S:EGDMA ratio by volume with interval time.

The EGDMA content also affected to the water adsorption capacity. As seen from Figure 4.11, there were two important reasons could explain these results. First, the water uptake increased due to hydrophilicity of ethylene glycol dimethacrylate. Secondly, flexibility of this crosslinking comonomer was resulting in more swelling of material leading to be capable of adsorption more water. In addition, the factor of pore size also might have affected for penetrating of water molecule. From these reasons above, the 60:40 S:EGDMA ratio poly(S/EGDMA)HIPE had the highest water adsorption capacity even it had low openness and interconnectivity pore structure.

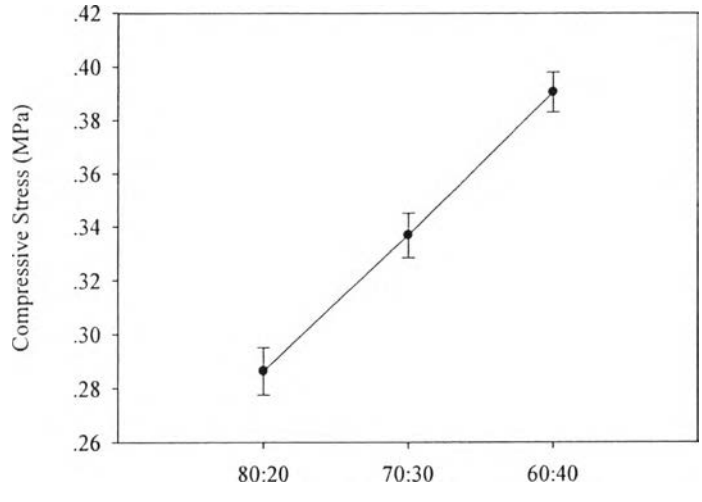

Figure 4.12 Compressive stress of poly(S/EGDMA)HIPEs varied S:EGDMA ratio.

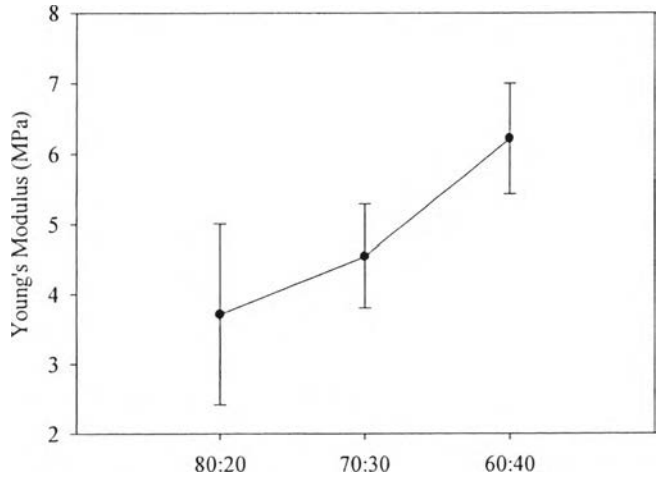

Figure 4.13 Young's modulus of poly(S/EGDMA)HIPEs varied S:EGDMA ratio.

Figure 4.12 and 4.13 shows the compressive stress and Young's modulus of poly(S/EGDMA)HIPEs varied S:EGDMA ratio, increasing in EGDMA content from 20% to 40% could enhance the Young's modulus from 3.7111 to 6.2147 MPa and compressive stress from 0.2864 to 0.3906 MPa. These results can explain that the increasing EGDMA content resulted in the increasing compressive stress and Young's modulus owing to the increases of degree of crosslinking.

4.3 Comparison of relative equilibrium water adsorption capacity between poly(S/DVB)HIPEs and poly(S/EGDMA)HIPEs

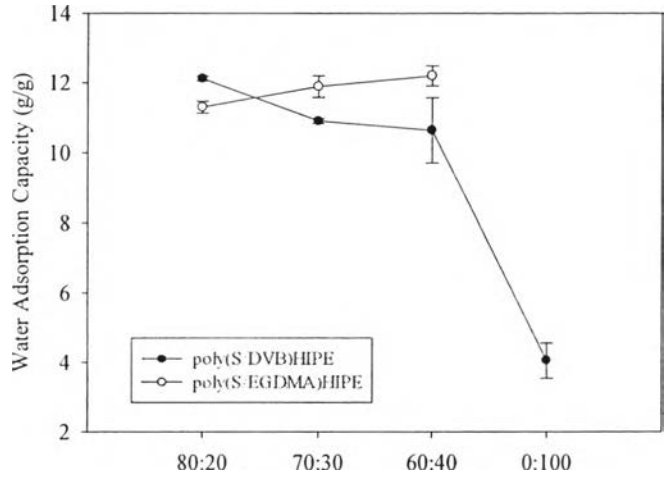

Figure 4.14 Relative equilibrium water adsorption capacity of poly(S/DVB)HIPEs and poly(S/EGDMA)HIPEs.

As seen from Figure 4.14, the ratio 70:30 polyHIPE of both systems showed similar porous structure (Figure 4.6b, 4.10b) and equal average pore diameter at 65 μm. Obviously, the water adsorption capacity of poly(S/EGDMA)HIPE was relatively higher than poly(S/DVB)HIPE. This result is owing to the more hydrophilicity and flexibility of EGDMA comonomer which provided more swelling of the structure. From this reason, poly(S/EGDMA)HIPE was able to adsorb more volume of water than poly(S/DVB)HIPE.